Ce^{3+} activated $LaBr_{3-x}I_x$: High-light-yield and fast-response mixed halide scintillators

M. D. Birowosuto,[1,a)] P. Dorenbos,[1,b)] K. W. Krämer, and H. U. Güdel
[1]*Radiation Detection and Matter, Faculty of Applied Sciences, Delft University of Technology, Mekelweg 15, 2629 JB Delft, The Netherlands*
[2]*Department of Chemistry and Biochemistry, University of Bern, Freiestrasse 3, 3000 Bern 9, Switzerland*

(Received 17 February 2008; accepted 28 March 2008; published online 22 May 2008)

Here, we report the scintillation properties of $LaBr_{3-x}I_x$:5%Ce^{3+} with four different compositions of x, i.e., x=0.75, 1.5, 2, and 2.25. Radioluminescence spectra reveal a shift of the emission wavelength with the $LaBr_3$ to LaI_3 ratio. $LaBr_{1.5}I_{1.5}$:5%Ce^{3+} shows the highest scintillation light yield of 58 000 photons/MeV, whereas $LaBr_{0.75}I_{2.25}$:5%Ce^{3+} shows the fastest scintillation decay time of 12 ns under 662 keV γ-ray excitation. This decay time is faster than that of 16 ns in $LaBr_3$:Ce^{3+}. The temperature dependence of radioluminescence spectra is presented. The structures and lattice parameters of the materials were determined from powder x-ray diffraction. © *2008 American Institute of Physics*. [DOI: 10.1063/1.2930884]

I. INTRODUCTION

The search for new scintillators remains important in the past decade because of demands in the fields of medical diagnostics, nondestructive testing, homeland security, and many fields of physics and chemistry. One of the searching grounds for new scintillators is halide compounds.[1] Eu^{2+} and Ce^{3+} activated barium halide scintillators were recently discovered for x-ray and γ-ray detections.[2,3] Light yields of these materials are lower than 20 000 photons/MeV and decay times are slower than 80 ns. Among all investigated halides, Ce^{3+} activated lanthanide trihalides are known as a scintillator family that often show high light yield and good energy resolution. One of its members, LuI_3:Ce^{3+}, is a scintillator with the highest scintillation light yield of 98 000 photons/MeV.[4]

In an attempt to search for better halide scintillators, we decided to investigate the scintillation and luminescence properties of mixed crystals of $LaBr_{3-x}I_x$:Ce^{3+}. $LaBr_3$:Ce^{3+} is a scintillator with a fast decay time of 16 ns and a high light yield of 70 000 photons/MeV.[5] LaI_3:Ce^{3+} does not emit photons at room temperature (RT), which is attributed to the autoionization of the 5*d* electron of Ce^{3+} to the conduction band. This autoionization of the 5*d* electron to the conduction band is related to the smaller band gap of 3.3 eV of LaI_3 than that of 5.9 eV of $LaBr_3$.[6,7] The lowest 5*d* state of Ce^{3+} in LaI_3 is only situated at 0.1–0.2 eV from the bottom of the conduction band.[6] With the mixed crystals, we anticipate that the band gap falls between the band gap of $LaBr_3$ and that of LaI_3. This could possibly increase the light yield of the mixed crystal, as compared to that of $LaBr_3$:Ce^{3+}.

An early investigation on the scintillation properties of Ce^{3+} activated $LaBr_{3-x}I_x$ with polycrystalline structure was previously reported by Glodo *et al.*[8] The 1% Ce^{3+} activated sample shows a light yield of 24 100 photons/MeV with an energy resolution of 7%. In this publication, we report the scintillation properties of 5% Ce^{3+} activated samples with improved crystal quality. The high light yield of 58 000 photons/MeV and the decay time of 12 ns are reported for these samples. This yield is competitive with 70 000 photons/MeV of $LaBr_3$:Ce^{3+} and this decay time is faster than 16 ns of $LaBr_3$:Ce^{3+}. Their crystal structures and lattice parameters were determined from powder x-ray diffraction (XRD).

II. EXPERIMENTAL METHODS

A. Crystal growth

Crystals of Ce^{3+} activated $LaBr_{3-x}I_x$ were grown by the Bridgmann method. The appropriate mixtures of $LaBr_3$, LaI_3, and $CeBr^3$ were sealed under vacuum in silica ampoules. Single crystals of four different compositions, i.e., $LaBr_{2.25}I_{0.75}$:5%Ce^{3+}, $LaBr_{1.5}I_{1.5}$:5%Ce^{3+}, $LaBrI_2$:5%Ce^{3+}, and $LaBr_{0.75}I_{2.25}$:5%Ce^{3+}, were obtained (see Fig. 1).

The color of the crystals changes with increasing LaI_3 concentration from colorless to yellow. $LaBr_{2.25}I_{0.75}$:5%Ce^{3+} is colorless as $LaBr_3$:Ce^{3+}. The hygroscopicity of the crystals increases with their LaI_3 contents too.

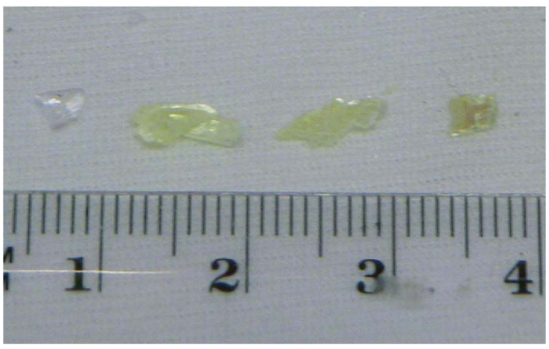

FIG. 1. (Color online) $LaBr_{3-x}I_x$:Ce^{3+} crystals with different Br/I ratios. They are $LaBr_{2.25}I_{0.75}$:5%Ce^{3+}, $LaBr_{1.5}I_{1.5}$:5%Ce^{3+}, $LaBrI_2$:5%Ce^{3+}, and $LaBr_{0.75}I_{2.25}$:5%Ce^{3+} from left to right, respectively.

[a)]Present address: Complex Photonic Systems, Faculty of Science and Technology, University of Twente, P.O. Box 217, 7500 AE, Enschede, The Netherlands. Electronic mail: m.d.birowosuto@utwente.nl.
[b)]Electronic mail: p.dorenbos@tudelft.nl.

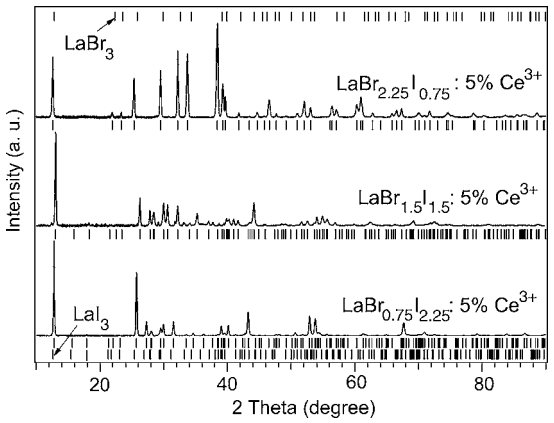

FIG. 2. XRD patterns of powder samples of $LaBr_{2.25}I_{0.75}$:5%Ce^{3+}, $LaBr_{1.5}I_{1.5}$:5%Ce^{3+}, and $LaBr_{0.75}I_{2.25}$:5%Ce^{3+} at RT. Calculated XRD line positions are shown as vertical lines (|) below the respective traces. Those of $LaBr_3$ (top) and LaI_3 (bottom) were obtained from Krämer *et al.* (Ref. 9) and Asprey *et al.* (Ref. 10), respectively.

The crystal growth of $LaBr_{3-x}I_x$:Ce^{3+} is difficult since $LaBr_3$ and LaI_3 differ in crystal structure. $LaBr_3$ has a UCl_3-type structure, space group $P6_3/m$ with a ninefold tricapped trigonal prismatic coordination of Br^- around La^{3+}, whereas LaI_3 has a $PuBr_3$-type structure, space group *Cmcm* with an eightfold bicapped trigonal prismatic coordination of I^- around La^{3+}.[9,10] The ionic radius of Br^-, 1.82 Å, is smaller than that of I^-, 2.06 Å.

B. XRD

XRD pattern of powder samples were measured on a Stoe STADI P diffractometer at RT. A Bragg–Brentano reflection geometry was used with α-SiO_2 (101) monochromated Cu $K\alpha_1$ radiation ($\lambda = 1.540\,598$ Å). The diffraction diagrams were recorded with a linear position-sensitive detector in a 2θ range of $10° - 100°$ or 150° with a resolution of 0.01°. Since the materials are hygroscopic, the powders were measured in a gas tight cell with a Mylar window.

C. Radioluminescence measurements

Radioluminescence spectra were recorded using an x-ray tube with Cu (XR) anode operating at 35 kV and 25 mA. The emission of the sample was dispersed by means of an Acton Research Corporation (ARC) VM-504 monochromator (blazed at 300 nm, 1200 groves/mm) and detected by a Hamamatsu R934-04 photomultiplier tube (PMT). The spectra were corrected for the wavelength dependence of the photodetector efficiency as well as the monochromator transmission.

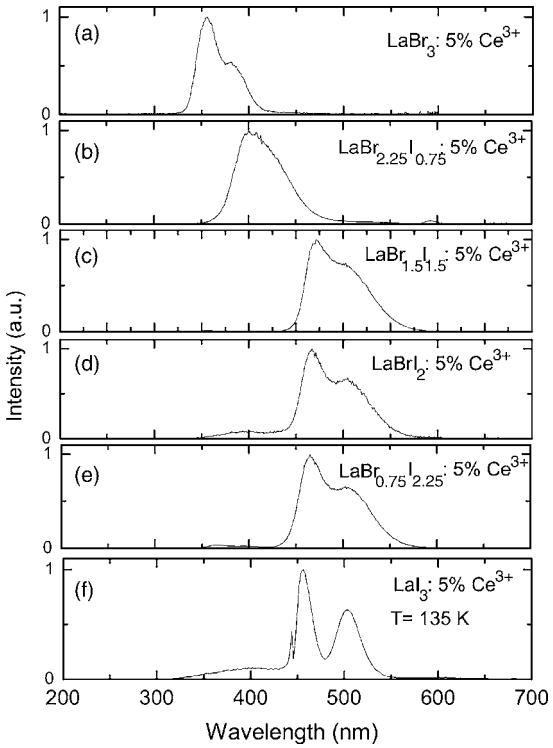

FIG. 3. Radioluminescence spectra of $LaBr_{2.25}I_{0.75}$:5%Ce^{3+}, $LaBr_{1.5}I_{1.5}$:5%Ce^{3+}, $LaBrI_2$:5%Ce^{3+}, and $LaBr_{0.75}I_{2.25}$:5%Ce^{3+} at RT. Emission spectra of $LaBr_3$:5%Ce^{3+} and LaI_3:5%Ce^{3+} recorded at RT and 135 K, respectively, are added for comparison.

D. Pulse height measurements

Pulse height spectra were recorded with a Hamamatsu R1791 PMT (cathode voltage=−600 V) with a box-type dynode structure connected to a preamplifier and an Ortec 672 spectroscopic amplifier. The crystals were mounted to the PMT window without an optical coupling and covered with several layers of Teflon tape for collection of scintillation light. The measurements were performed inside an M-Braun UNILAB dry box with a moisture content less than 1 ppm. The yield Y_{pe}, expressed in photoelectrons/MeV of absorbed γ-ray energy, was obtained by comparison of the peak position of the 662 keV photopeak relative to the position of the single-photoelectron peak. The absolute photon yield Y_{ph} in photons per MeV is derived from Y_{pe} as follows:[11]

TABLE I. Lattice parameters, calculated densities ρ_{cal}, and effective atomic numbers Z_{eff} of $LaBr_{2.25}I_{0.75}$:5%Ce^{3+}, $LaBr_{1.5}I_{1.5}$:5%Ce^{3+}, $LaBrI_2$:5%Ce^{3+}, and $LaBr_{0.75}I_{2.25}$:5%Ce^{3+} at RT. The values for $LaBr_3$ and LaI_3 were obtained from Krämer *et al.* (Ref. 9) and Asprey *et al.* (Ref. 10), respectively.

$LaBr_{3-x}I_x$	Space group	a (Å)	b (Å)	c (Å)	ρ_{cal} (g/cm^3)	Z_{eff}
$LaBr_3$	$P6_3/m$	7.9648(5)	$=a$	4.5119(5)	5.07	46.90
$LaBr_{2.25}I_{0.75}$:5%Ce^{3+}	$P6_3/m$	8.111(1)	$=a$	4.5392(4)	5.47	48.79
$LaBr_{1.5}I_{1.5}$:5%Ce^{3+}	*Cmcm*	4.3297(5)	13.561(1)	9.698(1)	5.51	51.45
$LaBrI_2$:5%Ce^{3+}	*Cmcm*	4.3105(7)	13.487(3)	9.647(2)	5.59	52.50
$LaBr_{0.75}I_{2.25}$:5%Ce^{3+}	*Cmcm*	4.3724(8)	13.8323(9)	9.904(1)	5.60	52.96
LaI_3	*Cmcm*	4.37(2)	14.01(2)	10.04(1)	5.61	54.20

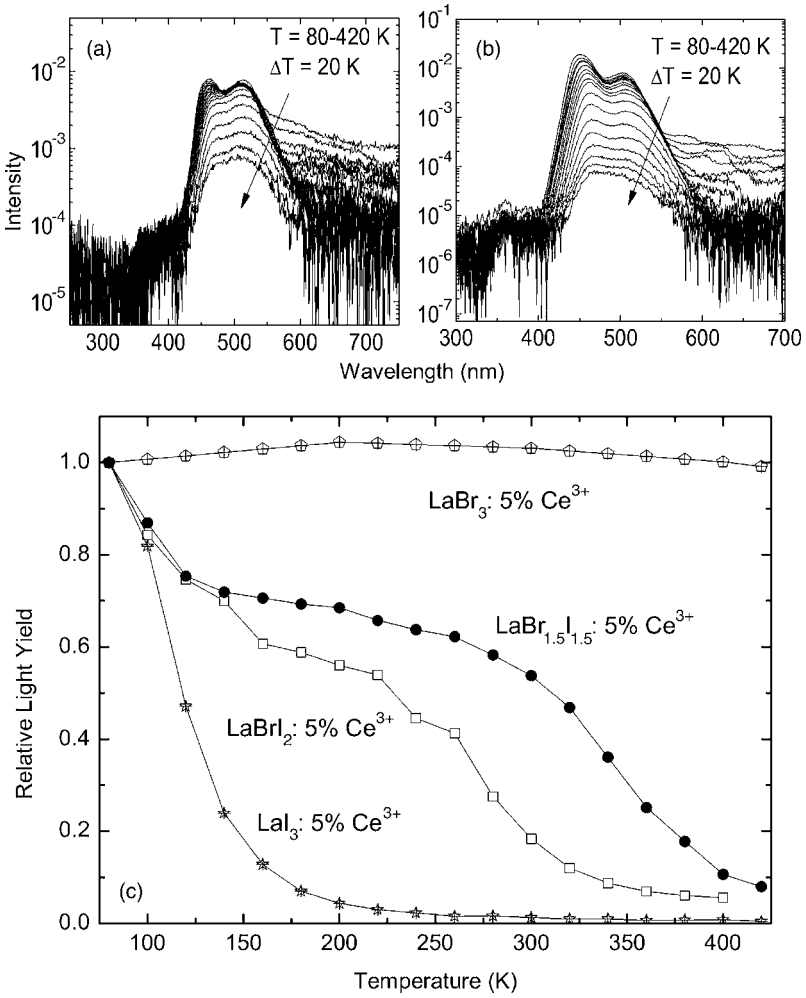

FIG. 4. Temperature dependence of radioluminescence spectra of (a) $LaBr_{1.5}I_{1.5}$:5%Ce^{3+} and (b) $LaBrI_2$:5%Ce^{3+} from 80 to 420 K with an interval of 20 K. The temperature increases along the directions indicated by arrows. (c) Temperature dependence of the radioluminescence spectra of $LaBr_{1.5}I_{1.5}$:5%Ce^{3+} and $LaBrI_2$:5%Ce^{3+}. Those of LaI_3:5%Ce^{3+} and $LaBr_3$:5%Ce^{3+} were added for comparison and obtained from Bessiere *et al.* (Ref. 6) and Bizarri *et al.* (Ref. 15), respectively. Relative light yields were obtained by normalizing each integral of the radioluminescence spectrum with that recorded at 80 K.

$$Y_{\mathrm{ph}} = Y_{\mathrm{pe}} \frac{1 - R_{\mathrm{eff}}}{R_{\mathrm{PTFE}} QE_{\mathrm{eff}}}, \tag{1}$$

where QE_{eff} is the effective quantum efficiency obtained from the manufacturer and R_{eff} is the PMT effective reflectivity previously measured by de Haas *et al.*[11] Both are averaged over the profile of the radioluminescence spectra. The reflection coefficient estimated for the 1 mm total thickness Teflon layer wrapping R_{PTFE} is 0.98.[12]

E. Scintillation decay measurements

Scintillation decay spectra were recorded using the single photon counting method.[13] The crystal inside a quartz ampoule was mounted on an XP2020Q PMT acting as the start PMT. The quartz ampoule was covered with layers of Teflon tape. We made a hole in the Teflon tape, which allows few scintillation photons to reach the second XP2020Q PMT acting as the stop PMT. For electronics, an Ortec 934 constant fraction discriminator, an Ortec 567 time to amplitude converter, and an AD413 CAMAC analog to digital converter were used.

III. RESULTS AND DISCUSSION

XRD patterns of $LaBr_{3-x}I_x$:Ce^{3+} are shown in Fig. 2. From these patterns, the structure types were determined and the lattice parameters were refined. The results are summarized in Table I. As $LaBr_3$, the $LaBr_{2.25}I_{0.75}$:5%Ce^{3+} crystallizes in the UCl_3 structure with space group $P6_3/m$. All other compounds with a higher LaI_3 content adopt the $PuBr_3$ structure with space group *Cmcm*.

The mass density ρ_{cal} in column 6 of Table I was calculated from the crystal structure. The effective atomic number Z_{eff} in column 7 of Table I depends on the Br^-/I^- ratio. The lattice parameters, ρ_{cal} and Z_{eff}, increase toward higher concentration.

Radioluminescence spectra of $LaBr_{3-x}I_x$:Ce^{3+} are shown in Fig. 3. All spectra are normalized to unity at the maximum of the emission spectra. All spectra are dominated by two bands assigned to the $5d \rightarrow 4f$ Ce^{3+} [$^2F_{5/2}$, $^2F_{7/2}$] doublet emission.

In $LaBr_{2.25}I_{0.75}$:5%Ce^{3+}, the Ce^{3+} doublet emissions are peaked at 400 and 434 nm [see spectrum (b) in Fig. 3]. This emission is shifted 44 nm to longer wavelength, as compared to the Ce^{3+} doublet emissions in $LaBr_3$:5%Ce^{3+} [see spectrum (a) in Fig. 3]. When the LaI_3 concentration increases to 50% (x=1.5), the Ce^{3+} doublet emissions are shifted to 472 and 500 nm [see spectrum (c) in Fig. 3]. If the concentration of LaI_3 is above 50%, the spectra are similar to that of $LaBr_{1.5}I_{1.5}$:5%Ce^{3+} [see spectra (d) and (e) in Fig. 3]. The Ce^{3+} doublet emissions in the LaI_3:5%Ce^{3+} emission spectrum recorded at 135 K are peaked at shorter wavelengths of 452 and 502 nm [see spectrum (f) in Fig. 3]. At RT, these

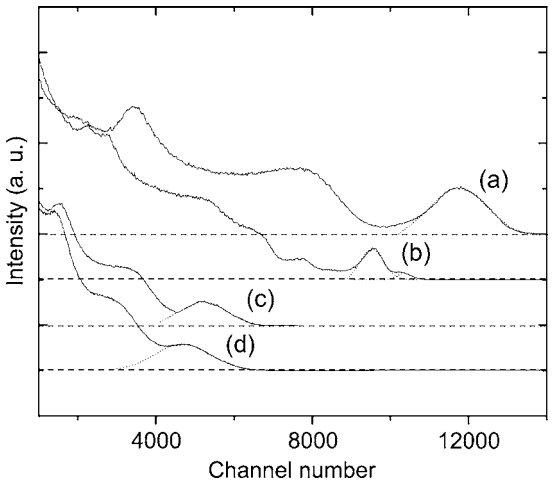

FIG. 5. Pulse height spectra under ^{137}Cs 662 keV γ-ray excitation of (a) $LaBr_{1.5}I_{1.5}$:5%Ce^{3+}, (b) $LaBr_{2.25}I_{0.75}$:5%Ce^{3+}, (c) $LaBrI_2$:5%Ce^{3+}, and (d) $LaBr_{2.25}I_{0.75}$:5%Ce^{3+} recorded with a Hamamatsu R1791 PMT and a shaping time of 10 μs. The dotted and the dashed lines correspond to Gaussian fits of the photopeaks and the background levels, respectively.

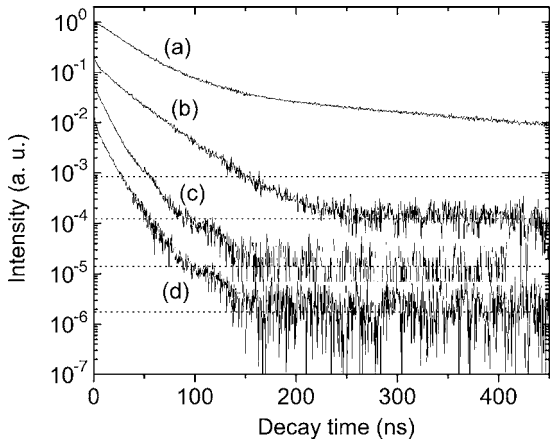

FIG. 6. Scintillation decay curves of (a) $LaBr_{2.25}I_{0.75}$:5%Ce^{3+}, (b) $LaBr_{1.5}I_{1.5}$:5%Ce^{3+}, (c) $LaBrI_2$:5%Ce^{3+}, and (d) $LaBr_{0.75}I_{2.25}$:5%Ce^{3+} recorded using the single photon counting method at RT. The dashed lines correspond to the background levels for each decay curve.

peaks may shift to the same wavelengths of those of Ce^{3+} doublet emission in $LaBr_{1.5}I_{1.5}$:5%Ce^{3+} but, unfortunately, Ce^{3+} doublet emission in LaI_3:5%Ce^{3+} is almost completely quenched at temperatures above 250 K.[6] The emission shift to longer wavelength with temperature increase was previously also observed in LuI_3:Ce^{3+} and was attributed to self-absorption effects.[14] Additionally, a weak broad band peaked at 390 nm is observed in spectra (d) and (e) in Fig. 3. This band can be assigned to the remnant of the self-trapped exciton emission, as previously observed in LaI_3:Ce^{3+} [see spectrum (f) in Fig. 3].[6]

Figure 4 shows temperature dependence of radioluminescence spectra of $LaBr_{1.5}I_{1.5}$:5%Ce^{3+} and $LaBrI_2$:5%Ce^{3+} and the integrated emission intensity as a function of temperature of $LaBr_3$:5%Ce^{3+}, $LaBr_{1.5}I_{1.5}$:5%Ce^{3+}, $LaBrI_2$:5%Ce^{3+}, and LaI_3:5%Ce^{3+}. The $5d \rightarrow 4f$ Ce^{3+} [$^2F_{5/2}$, $^2F_{7/2}$] doublet emission is well resolved in the emission spectra of $LaBr_{1.5}I_{1.5}$:5%Ce^{3+} and $LaBrI_2$:5%Ce^{3+} at 80 K [see Figs. 4(a) and 4(b)]. The origin of the band located around 600 nm at low temperatures is not clear. With the increase of temperature, the contribution from both Ce^{3+} emission band and the band peaked at 600 nm decreases.

The integrated radioluminescence intensity as a function of temperature is shown in Fig. 4(c). There is no decrease in light yield for $LaBr_3$:5%Ce^{3+} from 80 to 420 K. When the LaI_3 concentration increases, one does observe quenching effects. At RT, $LaBr_{1.5}I_{1.5}$:5%Ce^{3+} and $LaBrI_2$:5%Ce^{3+} show light yields of 54% and 18%, respectively, compared to the yield at 80 K, whereas LaI_3:5%Ce^{3+} shows no luminescence at all.

Figure 5 shows the ^{137}Cs source pulse height spectra of $LaBr_{3-x}I_x$:5%Ce^{3+}. Light yields derived from the pulse height spectra are listed in Table II. The energy resolution R (full width at half maximum over the photopeak position) is obtained from the Gaussian fit of the photopeak. For the $LaBr_{2.25}I_{0.75}$:5%Ce^{3+} pulse height spectrum, we observe two photopeaks [see spectrum (b) in Fig. 5]. This is probably due to two regions in the crystals, which give two different light yields. Therefore, two light yields and energy resolutions of $LaBr_{2.25}I_{0.75}$:5%Ce^{3+} are listed in Table II.

Table II shows that the light yield does not change much when applying different shaping times and, therefore, the decay times are shorter than or equal to 500 ns. The highest light yield of 58 000 photons/MeV is found for $LaBr_{1.5}I_{1.5}$:5%Ce^{3+}. The light yield at 10 μs shaping time decreases abruptly when x increases from 1.5 to 2 (see column 5 in Table II).

Scintillation decay curves of $LaBr_{3-x}I_x$:5%Ce^{3+} are shown in Fig. 6. The decay curves were recorded using the single photon counting method at RT under ^{137}Cs γ-ray excitation.[13] The decay curve for $LaBr_{2.25}I_{0.75}$:5%Ce^{3+} has been fitted with two exponentials, whereas the other decay curves with a single exponential.

TABLE II. Photoelectron yield, light yield, and energy resolution derived from pulse height spectra of $LaBr_{3-x}I_x$:5%Ce^{3+} under 662 KeV γ-ray excitation measured with a Hamamatsu R1791 PMT using shaping time of 0.5 and 10 μs, and characteristic components of the scintillation decay curves. Values in the table have errors of $\pm 10\%$.

Compound $LaBr_{3-x}I_x$	Photoelectron (10^3 photoelectrons/MeV) 0.5 μs	10 μs	Light yield (10^3 photons/MeV) 0.5 μs	10 μs	Energy resolution (%)	Decay components (relative contribution to total light yield) ns (%)
$LaBr_{2.25}I_{0.75}$:5%Ce^{3+}	13.8	14.9	42	45	4.1	31 (70), 244 (30)
	12.7	13.7	38	41	7.3	
$LaBr_{1.5}I_{1.5}$:5%Ce^{3+}	15.9	16.9	55	58	14.6	28 (100)
$LaBrI_2$:5%Ce^{3+}	6.6	7.5	22	25	25.9	13 (100)
$LaBr_{0.75}I_{2.25}$:5%Ce^{3+}	6.6	6.7	22	22	35.9	12 (100)

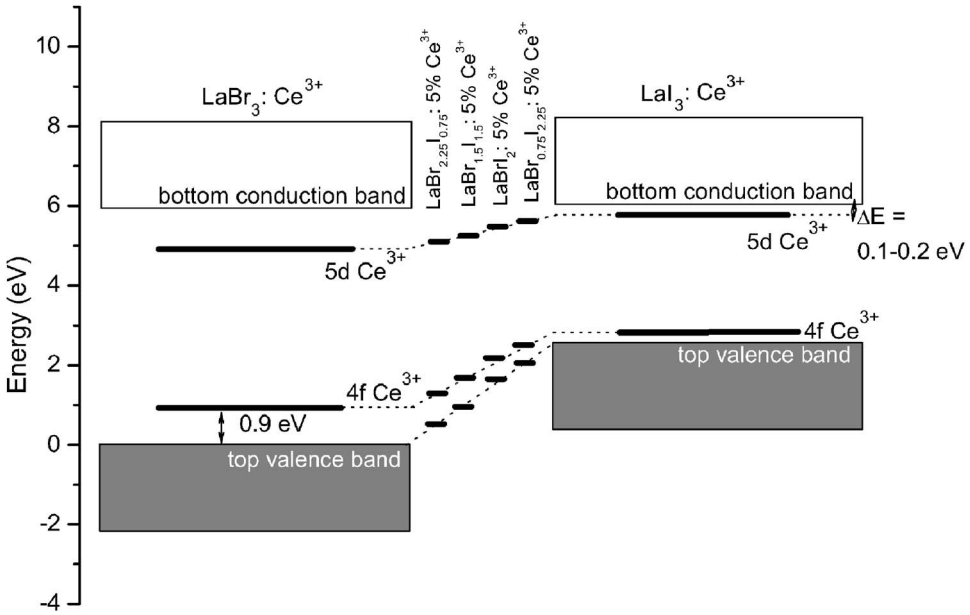

FIG. 7. Energy level schemes of $LaBr_3:Ce^{3+}$, $LaBr_{3-x}I_x:Ce^{3+}$, and $LaI_3:Ce^{3+}$.

Decay components with their relative contribution to the total light yield are presented in Table II. $LaBr_{2.25}I_{0.75}:5\%Ce^{3+}$ decay curve shows a fast component of 31 ns and a slow component of 244 ns. The fast component is 15 ns slower than the 16 ns intrinsic Ce^{3+} emission decay time of $LaBr_3:5\%Ce^{3+}$.[15] The presence of the slow component suggests a slow transfer of excitation energy from the host lattice to Ce^{3+}. This component disappears at higher LaI_3 concentration and the fastest decay component of 12 ns was recorded for $LaBr_{0.75}I_{2.25}:5\%Ce^{3+}$.

The fast decay times of 13 and 12 ns and the low light yields of 25 000 and 22 000 photons/MeV were observed in $LaBrI_2:5\%Ce^{3+}$ and $LaBr_{0.75}I_{2.25}:5\%Ce^{3+}$, respectively. The decay times are 2–3 ns faster than 15 ns of $LaBr_3:Ce^{3+}$, whereas the light yields are 45 000–48 000 photons/MeV of $LaBr_3:Ce^{3+}$.[15] In the integrated x-ray excited emission intensity as a function temperature, light yield of $LaBr_{3-x}I_x:Ce^{3+}$ decreases as the temperature increases. Here, we will discuss the possible cause of these reduced decay times and light yields. We envisage a model for the thermal quenching of Ce^{3+} emission and estimate the position of the Ce^{3+} emitting level relative to the conduction and valence bands in $LaBr_{3-x}I_x$.

The energy level schemes of $LaI_3:Ce^{3+}$, $LaBr_3:Ce^{3+}$, and $LaBr_{3-x}I_x:Ce^{3+}$ are shown in Fig. 7. The schemes of $LaI_3:Ce^{3+}$ and $LaBr_3:Ce^{3+}$ have been constructed with the information on the host lattice excitation and $4f \rightarrow 5d$ excitations from Bessiere *et al.*[6] and Dorenbos *et al.*,[7] respectively. The top of the bromide valence band is defined as zero of energy, whereas the top of the iodide valence band is located at 2.60 ± 0.15 eV. The bottom of the conduction bands of $LaBr_3$ and LaI_3 are located at 5.90 ± 0.15 eV. The energy differences between the lowest $4f$ and lowest $5d$ states of Ce^{3+} (E_{fd}) of $LaBr_3$ and LaI_3 are 4.03 ± 0.15 and 2.90 ± 0.15 eV, respectively.

In $LaBr_3:Ce^{3+}$, the $4f$ ground state of Ce^{3+} is located at 0.90 ± 0.40 eV above the valence band.[7] This value together with E_{fd} of $LaBr_3:Ce^{3+}$ locates the $5d$ state of Ce^{3+} at 4.93 ± 0.43 eV above the valence band. The lowest $5d$ state of Ce^{3+} is then at ~1 eV below the bottom of the conduction band. This large energy difference is consistent with the absence of Ce^{3+} emission quenching in $LaBr_3$ even at a temperature of 600 K.[15]

In $LaI_3:Ce^{3+}$, quenching of Ce^{3+} emission is due to the autoionization of an electron of the $5d$ Ce^{3+} to the conduction band because of the 0.1–0.2 eV small energy difference of the lowest $5d$ state of Ce^{3+} with the conduction band.[6] Lifetime shortening and light yield loss in $LaBr_{3-x}I_x:Ce^{3+}$ when the temperature increases can be associated with the thermal luminescence quenching model in $LaI_3:Ce^{3+}$. In the case of $LaBr_{3-x}I_x:Ce^{3+}$, we expect that the difference of the lowest $5d$ state of Ce^{3+} with the conduction band is larger than 0.2 eV but smaller than that in $LaBr_3$. This difference decreases toward high LaI_3 concentration. This assumption is based on the thermal quenching process from 150 to 450 K in the temperature dependence of integrated radioluminescence spectra of $LaBr_{3-x}I_x:Ce^{3+}$ (see Fig. 4). However, we cannot derive the activation energies for $LaBr_{3-x}I_x:Ce^{3+}$ from the integrated intensity curves. The thermal quenching from 80 to 150 K in the curves of $LaBrI_2:5\%Ce^{3+}$ and $LaBr_{1.5}I_{1.5}:5\%Ce^{3+}$ can be associated with other quenching mechanisms.

IV. CONCLUSION

Ce^{3+} activated $LaBr_{3-x}I_x$ crystals were grown by the Bridgmann method. XRD patterns of crystals show that $LaBr_{3-x}I_x:Ce^{3+}$ crystals are of single phase. $LaBr_{2.25}I_{0.75}:5\%Ce^{3+}$ has a UCl_3 crystal structure with space group $P6_3/m$, whereas $LaBr_{1.5}I_{1.5}:5\%Ce^{3+}$, $LaBrI_2:5\%Ce^{3+}$ and $LaBr_{0.75}I_{2.25}:5\%Ce^{3+}$ have a $PuBr_3$ crystal structure with space group *Cmcm*. The scintillation properties of Ce^{3+} activated mixed halides $LaBr_{3-x}I_x$ were also studied. The highest light yield of 58 000 photons/MeV was found for $LaBr_{1.5}I_{1.5}:5\%Ce^{3+}$, whereas the fastest decay time of 12 ns was found for $LaBr_{0.75}I_{2.25}:5\%Ce^{3+}$. The lower light yield and the faster decay time toward higher LaI_3 concentration

are assigned to the quenching of Ce^{3+} emission, which is due to autoionization of the Ce^{3+} $5d$ electron to the conduction band.

Since $LaBr_{3-x}I_x:Ce^{3+}$ crystals have relatively high light yield and fast response, the application for γ-ray and x-ray detection is very promising. The 0.40–0.53 g/cm^3 higher mass density than 5.07 g/cm^3 of $LaBr_3:Ce^{3+}$ is the advantage of $LaBr_{3-x}I_x:Ce^{3+}$. This means that $LaBr_{3-x}I_x:Ce^{3+}$ is better than $LaBr_3:Ce^{3+}$ with respect to high-energy detection efficiency. The energy resolution of $LaBr_{3-x}I_x:Ce^{3+}$ is rather poor, and the pulse height spectrum of $LaBr_{2.25}I_{0.75}:5\%Ce^{3+}$ even shows two photopeaks. Apparently, some part of $LaBr_{3-x}I_x:Ce^{3+}$ crystals produce more photons or photons are collected more efficiently from one part than from another part due to crystal inhomogeneity. An improvement in the technology of $LaBr_{3-x}I_x:Ce^{3+}$ crystal growth may bring $LaBr_{3-x}I_x:Ce^{3+}$ into a superior scintillator with a high light yield, good energy resolution, fast response, and high mass density.

ACKNOWLEDGMENTS

These investigations were supported by the Netherlands Technology Foundation (STW), the Swiss National Science Foundation, and Saint Gobain Crystals and Detectors, France.

[1] P. Dorenbos, Phys. Status Solidi A **202**, 195 (2005).
[2] J. Selling, M. D. Birowosuto, P. Dorenbos, and S. Schweizer, J. Appl. Phys. **101**, 034901 (2007).
[3] J. Selling, S. Schweizer, M. D. Birowosuto, and P. Dorenbos, J. Appl. Phys. **102**, 074915 (2007).
[4] M. D. Birowosuto, P. Dorenbos, C. W. E. van Eijk, K. W. Krämer, and H. U. Güdel, J. Appl. Phys. **99**, 123520 (2006).
[5] E. V. D. van Loef, P. Dorenbos, C. W. E. van Eijk, K. W. Krämer, and H. U. Güdel, Appl. Phys. Lett. **79**, 1573 (2001).
[6] A. Bessiere, P. Dorenbos, C. W. E. van Eijk, K. W. Krämer, H. U. Güdel, C. de Mello Donega, and A. Meijerink, Nucl. Instrum. Methods Phys. Res. A **537**, 22 (2005).
[7] P. Dorenbos, E. V. D. van Loef, A. P. Vink, E. van der Kolk, C. W. E. van Eijk, K. W. Krämer, H. U. Güdel, W. M. Higgins, and K. S. Shah, J. Lumin. **117**, 147 (2006).
[8] J. Glodo, E. V. D. van Loef, W. M. Higgins, W. W. Moses, S. E. Derenzo, and K. S. Shah, in Proceedings of the Eight International Conference on Inorganic Scintillators and Their Use in Scientific and Industrial Applications, Alushta, Crimea, Ukraine, 19–23 September 2005, edited by A. Gektin and B. Grinyov (National Academy of Sciences of Ukraine, Kharkov, 2006), p. 118.
[9] K. W. Krämer, T. Schleid, M. Schulze, W. Urland, and G. Meyer, Z. Anorg. Allg. Chem. **575**, 61 (1989).
[10] L. B. Asprey, T. K. Keenan, and F. H. Kruse, Inorg. Chem. **3**, 1137 (1964).
[11] J. T. M. de Haas, P. Dorenbos, and C. W. E. van Eijk, Nucl. Instrum. Methods Phys. Res. A **537**, 97 (2005).
[12] V. R. Weidner and J. J. Hsia, J. Opt. Soc. Am. **71**, 856 (1981).
[13] L. M. Bollinger and G. E. Thomas, Rev. Sci. Instrum. **32**, 1044 (1961).
[14] M. D. Birowosuto, P. Dorenbos, J. T. M. de Haas, C. W. E. van Eijk, K. W. Krämer, and H. U. Güdel, J. Lumin. **118**, 308 (2006).
[15] G. Bizarri and P. Dorenbos, Phys. Rev. B **75**, 184302 (2007).